PCCP

Accepted Manuscript

Volume 18 | Number 1 | 7 January 2016 | Pages 1–636

PCCP

Physical Chemistry Chemical Physics
www.rsc.org/pccp

ISSN 1463-9076

ROYAL SOCIETY OF CHEMISTRY

PERSPECTIVE
Darya Radziuk and Helmuth Möhwald
Ultrasonically treated liquid interfaces for progress in cleaning and separation processes

175 YEARS

ROYAL SOCIETY OF CHEMISTRY

rsc.li/pccp

H-Bonding Controls the Emission Properties of

Functionalized Carbon Nano-dots

Soumalya Mukherjee1, Edamana Prasad2*, and Anju Chadha 1,3*

1 Laboratory of Bioorganic Chemistry, Department of Biotechnology, Indian Institute of Technology

Madras, Chennai 600 036, India.

2 Department of Chemistry, Indian Institute of Technology Madras, Chennai 600 036, India

3National Centre for Catalysis Research, Indian Institute of Technology Madras, Chennai 600 036, India.

*Edamana Prasad. Tel:+91 44 2257 4232. E-mail: pre@iitm.ac.in

*Anju Chadha. Tel: 91-44-2257-4106. E- mail: anjuc@iitm.ac.in

ESI available.

ABSTRACT

Bathochromic and hypsochromic shifts in the photo-luminescent spectra of doped and functionalized carbon nano-dots (CD) arise due to the complex interaction between CD and the solvent molecules around them. Nitrogen-functionalized carbon nano-dots (N-CD) were synthesized from citric acid and urea using microwave assisted hydrothermal methods. Optical studies (absorption and photoluminescence) from the as-synthesized N-CD were carried out in polar protic, aprotic and non-polar solvents. When excited at 355 nm, blue photoluminescence (PL) was observed from N-CD dispersed in polar aprotic solvents while a green emissionwas observed in polar protic solvents. In addition to the general solvent effect, analysis of the luminescence spectra in protic solvents suggests that hydrogen bonding plays a crucial role in regulating the photophysical characteristics of the system. Temperature dependent PL studies and time correlated single photon counting experiments in various solvent dispersions of N-CD support the role of hydrogen bonding. This indicates that these results depend on the specific interactions observed from the N-CD and can be sought to be the primary driving force which is then followed by solvent properties like dipole moments. Both Lippert- Mataga model and Kamlet- Taft's parameters were used to support the photophysical properties observed from N-CD.

1. INTRODUCTION

Luminescent carbon based nano- dots (CD) and graphene quantum dots (GQD) have attracted significant attention in recent years due to their potential role in bio- imaging, bio-sensing, and photovoltaics[1-4]. While most of the CD emit in the visible region of the electromagnetic spectra, deep UV emitting graphene quantum dots (GQD) have also been realized in a recent study[5,6]. Unlike classical fluorophores, the emission peaks of CD and GQD are found to be dependent on the excitation wavelength[7-9].There are several reports, which have been reviewed recentlyon the study of the origin of the excitation dependent emission where intrinsic properties of CD play an important role in determining the emission wavelength[7].

In addition to this, the emission wavelength from the CD is also dependent on extrinsic parameters such as dopants and solvents[8,9]. Doping of the nano-dots are often carried out with hetero-atoms like nitrogen (N-CD) and sulphur (S-CD), which manipulate the band gap in the CD that subsequently leads to excitation dependent emission[10,11]. Similarly, when readily dispersed in polar solvents (stable dispersion due to presence of carboxylic, hydroxyl, carbonyl groups) complex interactions between the CD and solvent play a key role in wavelength dependent photoluminescence. Depending on the dipole moment of the solvents used to disperse the carbon nano-dots, a shift in the photoluminescence peak was reported with polar solvents[9]. The extent of this shift is a function of the rates of fluorescence relaxation of the excited electrons and the dipole rearrangement of the solvent molecules, often termed as the 'red-edge' effect[12,13]. Owing to these non- specific interactions between the solvent and the fluorophores, Lippert Mataga model was used to quantify these spectral shifts[14]. However, recent studies have reported the role of specific interactions such as hydrogen bonding on the photoluminescence (PL) of the nano-dots[15,16]. The violation of the classical Kasha- Vavilov's rule in these

carbon based quantum dots is often attributed to specific interactions (hydrogen bonds). Due to the presence of such (hydrogen bonding) interactions between the fluorophore and the polar protic solvents, Lippert-Mataga model may fail to account for the specific solvent-N-CD interactions and their effect on the PL characteristics[17].

This issue is addressed in the present study where Kamlet-Tafts parametersare used to explain the complex interactions that may take place between carbon nano-dots and the solvent molecules in their milieu. Such interactions are responsible for the spectral shifts in both UV absorption and PL spectra of the nano-dots.To validate the application of the Kamlet-Tafts parameters, temperature dependent photoluminescence and lifetime studies were carried out in solvents of different dielectric constants.

2. EXPERIMENTAL

The N-CD was synthesized by the bottom-up hydrothermal process where citric acid and urea were used as carbon and nitrogen sources respectively.To enhance the extent of hydrogen bonding interactions between the carbon nano-dots and polar solvents, nitrogen functionalized carbon nano-dots (N-CD) were chosen for our experiments.Given the fact that microwave assisted hydrothermal method (MWAH) gives the proper control over the size of the N-CD, it was used for the synthesis starting from citric acid and urea, details of which are included in the supporting information (S1)[18]. MWAH treatment of the aqueous mixture of the precursor materials results in both inter-molecular and intra-molecular condensation reactions, leading to the formation of functionalized carbon nano-dots by carbonization, wherein a proper control over their size can be sought[18,19]. Solid-state N-CD were procured from the aqueous dispersion via lyophilization which were then dispersed in various solvents (polar protic, aprotic and non-polar solvents), illustrated in the Supporting Information (S2). Characterization techniques like Transmission Electron Microscopy (TEM), X-ray diffraction (XRD), Fourier Transform Infra-red (FTIR), UV-

Visible spectroscopy and PL- spectroscopy were employed to study the morphological, chemical and the optical properties of the N-CD (S3).

3. RESULTS AND DISCUSSION

3.1 Characterization of the as-synthesized N-CD.

Transmission electron microscopy (TEM) images of aqueous dispersion of N-CD reveal the formation of circular carbon as shown in Fig. 1a.Statistical analysis revealed a narrow size distribution of N-CDs with an average diameter of about ~16 nm, as shown in Fig. 1(c).The shape and size of the dots did not change even when dispersed in ethyl acetate (Fig. 1c and Fig. 1d). The functional groups integrated in the structure of the N-CD were studied by FTIR (Fig. S1a) which revealed the presence of hydroxyl (3421 cm^{-1}), carboxyl (a broad peak at 2400 cm^{-1} and 3400 cm^{-1}), carbonyl (1613 cm^{-1}) and amine groups (3209 cm^{-1})[18-20]. Fig. S1b depicts the XRD spectrum of the as-synthesized N-CD. A small, broad peak at 2θ= 26.1° was observed corresponding to the (002) diffraction pattern of graphitic carbon[21]. This correlates to an inter-layer spacing of about 0.33 nm which is larger than the spacing of bulk graphite structures, presumably due to the incorporation of oxygen and nitrogen containing functional groups along the edges and on the surface of the N-CD.
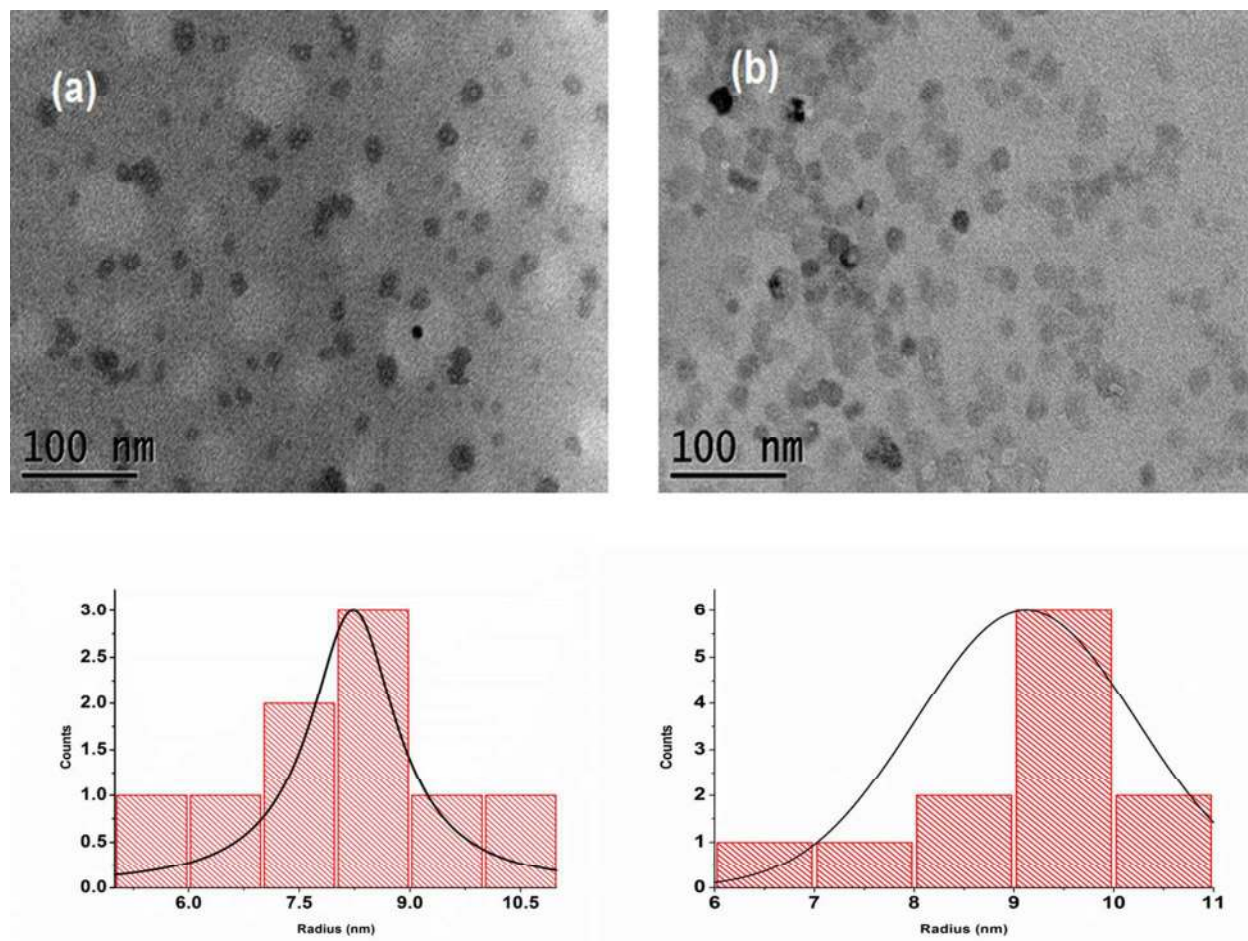
Fig.1. Transmission Electron Microscopy (TEM) image of N-CD dispersed in (a) water and (b) ethyl acetate. Distribution of size of N-CDs dispersed in (c) water and (d) ethyl acetate.

3.2 Photophysical studies of the nitrogen functionalized carbon nano-dots

Optical studies of the N-CD were carried out by analyzing their absorption and emission spectra. Organic compounds analogous to extended systems of benzene derivatives (carbon nano-dots) show strong absorbance in the UV region[22]. However, a spectral shift or a change in the intensities of such peaks gives us an idea about the interaction between the fluorophore and the solvents[22].Absorption spectra of the N-CD, dispersed in the different solvents, were obtained over a broad band of wavelength

ranging from 200 nm to 600 nm. When dispersed in water, the N-CD exhibit absorption peaks at 232 nm, 270 nm, 342 nm and a shoulder region over 400 nm as illustrated in Fig. 2a. An increase in optical absorption with increasing concentration was observed, which is consistent with previous studies[23].The peaks at 230 nm and 270 nm suggests the formation of delocalized π states as the former corresponds to the π-π* transitions of the C-C bonds in the carbon nano-dots, while the latter can be attributed to transitions of the sp^2 carbon domains that matches well with the transition energy of graphene sheets [24,25]. According to Reckmeier *et al.,* the peak at ~ 340 nm corresponds to the n- π* transitions arising from the edge states formed at the boundary of the sp^2 and the sp^3 hybridized carbons [26]. Such transitions (specifically associated with the lone pairs over carbonyl oxygen) involve the excitation of the electrons from their ground state to non-bonding orbitals. The low absorption at ~ 400 nm is often associated to the surface states, arising from the hydroxyl, carboxyl, amino and amide groups present at the edges of the carbon nano-dots[26].

On dispersing the lyophilized N-CD in different solvents, spectral shifts accompanied by a change in their intensities were observed. Such bathochromic or hypsochromic shifts are recorded in Table 1, while the resulting spectra are shown in Fig. 2b.
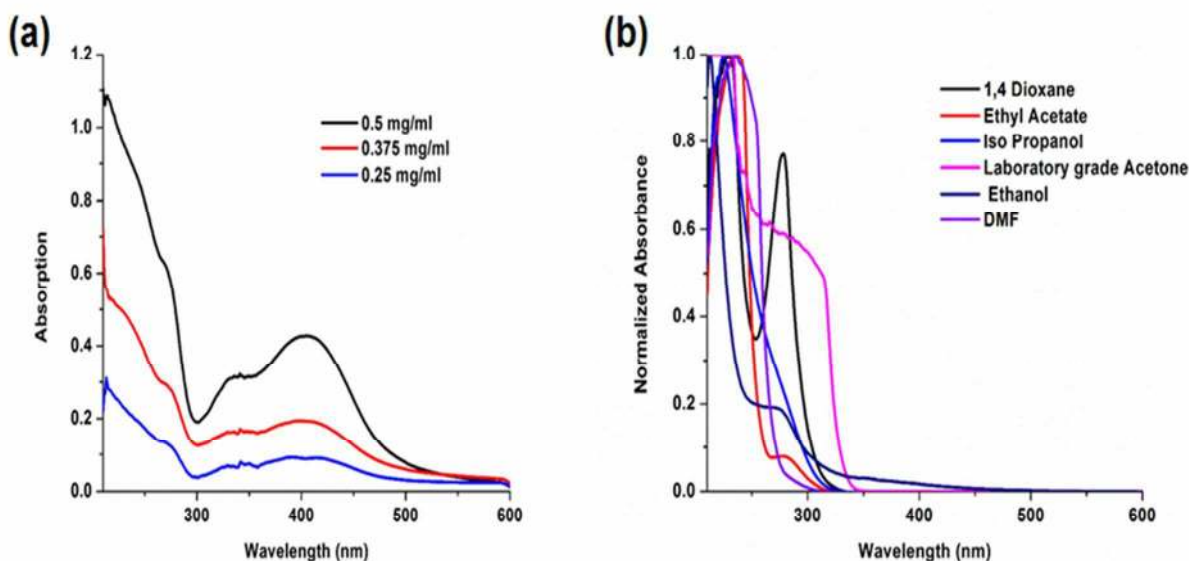
Fig. 2: (a) Absorption spectra of varying concentrations of N-CDs dispersed in water. Increase in the intensity of absorption with higher concentration was observed. (b) UV- Visible spectra of N-CDs dispersed in non-polar and polar (protic and non protic) solvents. Spectral shifts were observed with different solvents which can be explained on the basis of interactions between the solvent and the N-CD.

3.2.1 Spectral shifts associated with the absorption of N-CD dispersed in different solvents

Detailed study of such ground state spectral shifts of N-CD in different solvents has not been reported and thus demands a systematic study. Solvents of varying di-electric constants were used to disperse these N-CD which are tabulated in their increasing order (di-electric constants) in Table 1, where α, β and π^* (Kamlet- Taft's parameters) signify the hydrogen bond donation acidity, hydrogen bond acceptance basicity and the polarizability of the solvents, respectively. λ_{max} denotes the absorption peak maximum exhibited by π-π^* transitions of N-CDs when dispersed in the respective solvents.

Absorption, in contrast to photoluminescence, is a very fast process and is terminated in a time scale of a few femtoseconds. Thus, slow processes such as solvent re-orientation in their ground and excited states do not contribute towards determining the electronic energy levels. However, fields arising due to the charge transfer between N-CD and solvent molecules (through hydrogen bonds in the system) play a

major role in absorption. Functional groups like hydroxyl, carboxyl, amine and amide, increases the electron density on the N-CD and are responsible for inter-molecular hydrogen bonds. This suggests that the changes in the dipole moments and the Onsager radius, arising from such charge transfers, play a role in the observed spectral shifts.

Solvent	Di-electric constant (ε)	Dipole moment (μ)	α	β	π*	$f(n)=\dfrac{n^2-1}{2n^2+1}$	λmax, (nm)
1,4-dioxane	2.25	0.45	0	0.37	0.49	0.20	229
n-butyl acetate	5.10	1.87	0	0.45	0.46	0.19	236
ethyl acetate	6.02	1.88	0	0.45	0.55	0.18	235
tetrahydrofuran	7.58	1.75	0	0.55	0.58	0.19	230
iso-propanol	17.9	1.66	0.84	0.90	0.52	0.18	224
acetone	20.7	2.85	0.08	0.48	0.62	0.18	Broad peak
ethanol	24.5	1.69	0.86	0.75	0.54	0.18	224
DMF	36.7	3.86	0	0.69	0.88	0.20	235
water	80.1	1.82	1.17	0.47	1.069	0.16	232

Table 1. Polar and non-polar solvents that were used to disperse the N-CDs tabulated in their increasing order of di-electric constants.

Assuming this carbon dot- solvent system as a di-atomic molecule, the difference in the energies due to the electron transitions in the excited and the ground state is given by the Lippert- Mataga model:

$$\Delta E = \frac{2f(n)}{a^3}(\mu_E - \mu_G)^2 \qquad (1)$$

where 'a' is the Onsager radius and $f(n) = \frac{n^2-1}{2n^2+1}$, having 'n' as the refractive index of the solvent. μ_E and μ_G are the dipole moments of the solvent molecules in their excited and ground states, respectively.As evident from Table 1, λ_{max} and f(n) are inversely related in non-polar and polar aprotic solvents, which is in accordance to the Lippert- Mataga model. This suggests that no specific interactions take place between N-CD and non-polar and polar aprotic solvents and the energy difference (ΔE) is a function of the redistribution function f(n), as illustrated in Fig. S2a.

However, complex interactions take place when polar protic solvent molecules are in the vicinity of the N-CD. Depending on the interaction of the solvent molecules and the various functional groups on the N-CD, the aqueous shell surrounding the nano-dot is not uniform, as has been illustrated in Fig. S2b. This can be explained as follows:fluorophores containing – NH_2 and –OH groups, which act as electron donors in their excited states, are stabilized by hydrogen bond acceptor solvents. This mediates the transfer of the electronic charge away from the functional groups[28].Conversely, in case of –C=O and –COOH groups, change in the electronic distribution in its excited state results in minimal hydrogen bonding and hence low stabilization of the excited state by the polar protic or aprotic solvents[29]. Since N-CD containsboth classes of functional groups, the spectral shifts associated with the maximum absorption are due to their combined effect.

Mathematically, the above hypothesis can be extended to complex systems such as the N-CD, wherein a wide spectrum of functional groups like amine, hydroxyl, epoxy and carbonyl groups are present. The net energy difference (ΔE) can be found out by combining the effective transitionenergies associated with carbonyl and the amine groups.

Thus, the net energy difference can be expressed as follows (details are provided in the Supplementary Information):

$$\Delta E = \frac{2f(n)}{a^3}\left(\mu^2_{E(carbonyl)} - \mu^2_{G(amine)}\right) + 2f(n)\left(\frac{\mu'^2_E}{a'^3}_{amine} - \frac{\mu'^2_G}{a'^3}_{carbonyl}\right) \qquad (2)$$

The first term of the above equation can be generalized as the electronic transitions taking between the intrinsic band gap of the N-CD while the second term is dependent on the effective radius of the fluorophore-solvent diatomic complex, that is a linear function of the hydrogen bond donor capacity 'α' of the solvent. Thus, the λ_{max}depends inversely on f(n) and is directly proportional to the 'α'. The spectral shift observed for N-CD in polar protic solvents can be explained using the above model. For example, increase in the α value for water, compared to that in ethanol or iso-propanol results in an increased λ_{max}, as shown in Table 1. Hydrogen bonds, being charge mediated interactions, are an inverse square function of the distance while an inverse cubic function is attributed to the dipole- dipole interactions[30]. Since the field of hydrogen bonds is much larger than the dipole interactions, it can be stated that hydrogen bonds are the primary driving forces in controlling the band gap of the carbon nano-dots, which is then further stabilized by dipole interactions.

3.3 Steady state photoluminescent studies of N-CD dispersed in different solvents

Photoluminescence, on the other hand,is comparatively a slow process and hence opens avenues for dipole relaxation of the solvent molecules surrounding the fluorophore[17]. Upon excitation at 355 nm, dispersions of N-CD in most of the polar aprotic dispersions show blue fluorescence, while green PL is observed in polar protic solvents. Steady state fluorescence of N-CD was obtained to study the occurrence of new emission peaks and Stoke's shifts induced by the solvent on the fluorophore.

The steady state emission spectra of N-CD in various solvents are given in Fig. 3. A general trend that included spectral narrowing at higher excitation wavelength, was observed in the excitation dependent emission spectra of the aqueous dispersion of N-CD, which is in accordance with the previous reports

(Fig.3a)[31-34].Emission spectra of N-CD in hygroscopic polar aprotic solvent (laboratory grade acetone) also showed a similar behavior (Fig. 3b). Conversely, N-CD in polar aprotic solvents (ethyl acetate and n-butyl acetate) did not exhibit excitation dependent emissionspectra (Fig. 3c). Comparing the emission behavior of N-CD at 360 nm for different solvents, a green shift can be seen in aqueous dispersion as compared to polar aprotic (ethyl acetate) solvent. This can be due to the stabilization of the Franck Condon excited state of N-CD (aqueous dispersion) by charge transfers mediated by hydrogen bonding which is not possible for polar aprotic solvents due to `minimal interactions. These observations suggest that hydrogenbonding between N-CD and protic solvents play a key role in regulating the PL in the system.
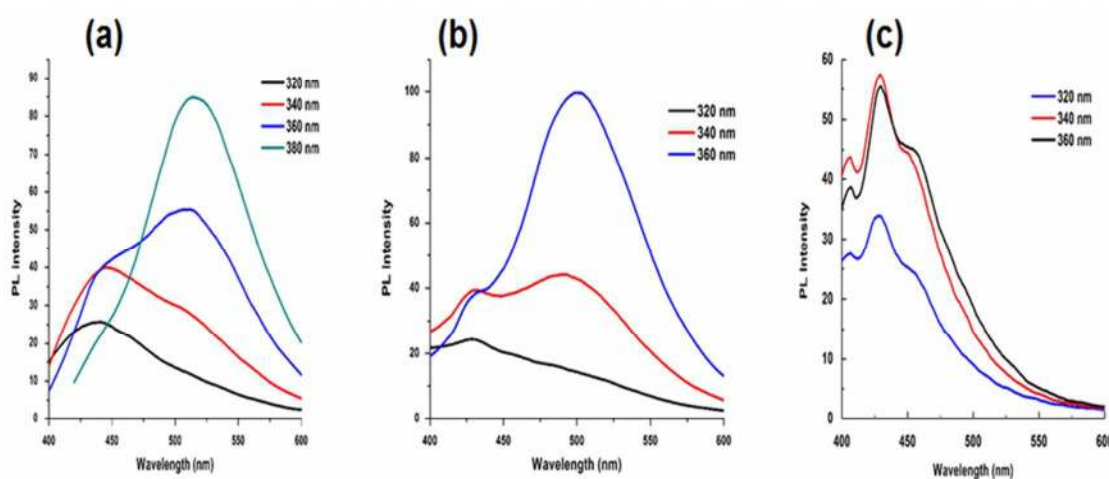

Fig. 3: Excitation dependent emission spectra exhibited by N-CDs dispersed in (a) polar protic solvent-water; (b) laboratory grade acetone. (c) ethyl acetate. The role of hydrogen bonding on the photophysical properties of N-CD can be anticipated.

Fig. S3a and Fig. S3b correlate the emission wavelength with their excitation energies obtained from N-CD dispersed in different solvents. Analysis of emission spectra at 340 nm and 400 nm is of particular interest. The former wavelength corresponds to the transitions at the edge states due to the sp^2 backbone of the carbon nano-dot and the sp^3 hybridized epoxy functional sites, whereas the later wavelength corresponds to the excitation of emissive traps arising from the surface functional groups[26].

Upon exciting the N-CD with energy equivalent to the edge state (340 nm), emission in blue region of the optical spectra (420 nm to 440 nm) was observed from all solvent dispersions. However, differences in emission wavelength arise at excitation wavelengths equivalent to the surface states (440 nm). N-CD dispersed in polar protic solvents show a green emission (~ 510 nm to 520 nm) while the aprotic dispersions still emit in the blue region (~ 470 nm),confirming the role of surface states in controlling the PL of N-CD. Since the surface states contain hydroxyl, amide, amine and carboxyl groups, the role of hydrogen bonds can be anticipated. This also suggests that specific interactions like hydrogen bonding do not hold for edge states, as minimal solvent interactions are anticipated here and hence Lippert-Mataga model can be used to explain the photophysics of these regions. However, Kamlet-Taft's parameters have to be used to study the emission spectra arising from the surface states as the spectra are vulnerable to interactions like hydrogen bonds.

Bathochromic shifts with increasing excitation wavelengths, obtained with polar protic solvent dispersions are attributed to the slow relaxation process of the solvent dipoles[12].Fundamentally,such solvation relaxation processes arise due to the reorganization of the solvent dipoles along the dipole moment of the excited electrons in the fluorophore. The extent of these red shifts depends on the polarity of the solvent, as highly polar molecules will induce stabilization of the lowest excited singlet state by strong dipole- dipole interaction[12]. Such dipole interactions are a composite function of the distance between the carbon nano-dots and the solvent molecules and hence, are dependent on specific interactions such as hydrogen bonding. In such cases, Kamlet-Taft parameters regulate the interactions between the N-CD and solvent molecules.

Minimal interaction through hydrogen bonding takes place when N-CDs are transferred to polar aprotic solvents like ethyl acetate and n- butyl acetate. Interestingly, when dispersed in laboratory-grade acetone, which is a polar aprotic solvent, these N-CDs exhibited a green fluorescence when excited at 350 nm. However, on dehydrating by the addition of sodium sulphate, a blue shift in their

emission was observed and exhibited excitation independent emission similar to ethyl acetate. This

change in the PL behavior isshown in Fig. S4a. Such observations coupled with the fact that acetone is

hygroscopic, supports the role of hydrogen bonding as the principle determinant of the

solvatochromism observed with N-CD in polar protic solvents.

3.4 Temperature dependent photo-luminescent studies of different solvent dispersions of N-CD

To confirm the effect of hydrogen bonding on the PL characteristics of N-CD, temperature dependent

photoluminescence and lifetime studies *via* time correlated single photon counting (TCSPC) were carried

out on four different dispersions of N-CDs. Solvents used in this study were water, ethyl

acetate(maximum water content < 0.1%), laboratory-grade (maximum water content ~ 5%)and

dehydrated acetone(maximum water content ~0.5%). The aqueous dispersion showed both excitation

and temperature dependent emission spectra as shown in Fig. 4a. Green shift of the emission spectra of

N-CD, when excited at 400 nm, along with a spectral narrowing was observed. Increase in the

temperature impedes the formation of hydrogen bonds between the N-CDs and the surrounding water

molecules, favoring faster solvent dipole re-orientation and greater stabilization of the Franck- Condon

excited state. Spectral narrowing at high temperatures suggests that the timescales of such

reorientation of solvent dipoles is lower than that at lower temperatures, leading to emission from a

fewer intermediate states.

In Fig. 4b, temperature independent emission spectra were observed from the N-CD in laboratory

grade acetone. Excitation dependent spectra was attributed to charge transfer taking place through

hydrogen bonds between the N-CDs and the surrounding aqueous shell formed by the water absorbed

by the hygroscopic solvent. Assuming low concentrations of water in this aprotic solvent, a slight

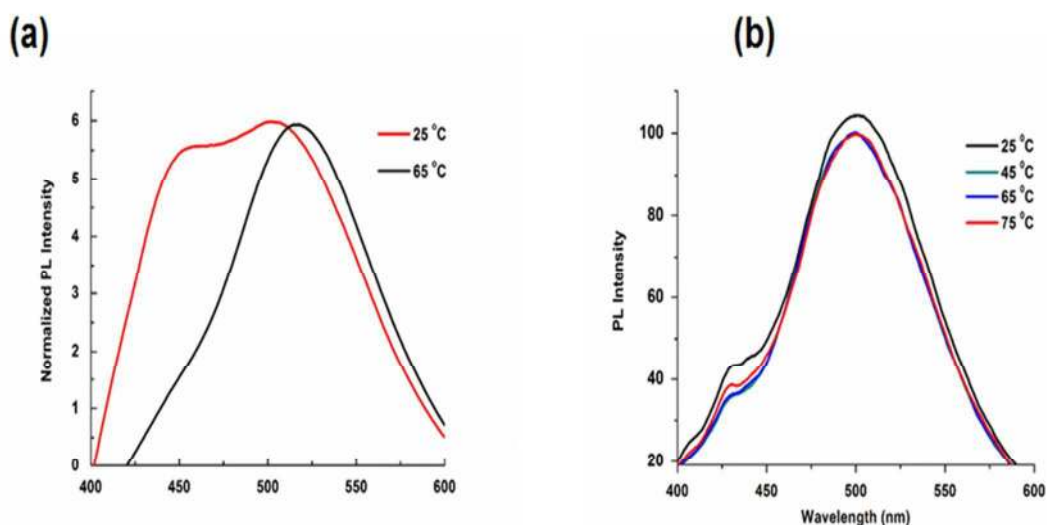increase in the temperature destabilizes the hydrogen bonds and disruptsthe aqueous shell.

Fig.4. Temperature dependent PL of N-CD dispersed in (a) water at an excitation wavelength of 400 nm. Green shift accompanied with spectral narrowing can be seen at 65 °C at an excitation wavelength corresponding to the surface states (b) acetone at an excitation wavelength of 400 nm at 25, 45, 65 and 75 ° showing no change.

Excitation and temperature independent PL was observed from N-CD dispersed in ethyl acetate and dehydrated acetone, as shown in the Fig. 5a to 5d. This temperature independent emission suggests the absence of any interaction between the N-CDs and aprotic solvents which subsequently confirms the hypothesis that these nano-dots are poor hydrogen bond donors, as has been reported by a recent study[17]. The variation in the Stoke's shifts exhibited by various dispersions of N-CDs (excitation wavelength of 400 nm) at different temperatures is tabulated in Table 2. A higher shift was observed in the presence of water as compared to the dehydrated aprotic solvents (like ethyl acetate) which confirms the solvent relaxation (or dipolar reorganization) of the surrounding water molecules in the former case.
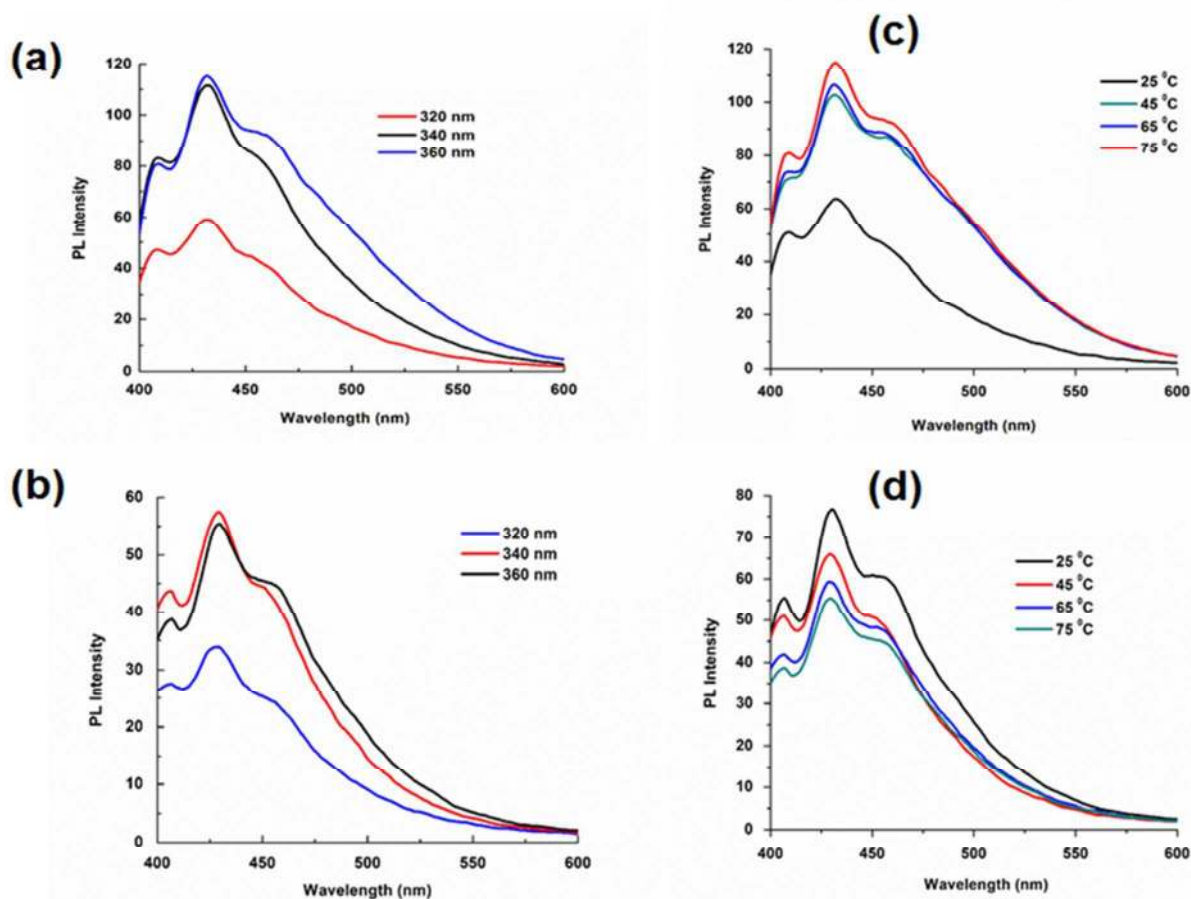
Fig. 5: Excitation independent photoluminescence emission of N-CDs dispersed in (a) acetone and (b) ethyl acetate. Emission spectra obtained at an excitation wavelength of 360 nm from N-CDs dispersed in (c) acetone and (d) ethyl acetate.Minimal interaction between the N-CD and the polar aprotic solvents can be anticipated from these studies.

Solvents	Temperature			
	25 ˚C	45 ˚C	65 ˚C	75 ˚C
Water	72 nm	130 nm	151 nm	153 nm
Acetone (dehydrated)	71 nm	73 nm	71 nm	71 nm
Laboratory-grade Acetone	138 nm	139 nm	138 nm	139 nm
Ethyl Acetate	71 nm	68 nm	69 nm	69 nm

Table 2. Stoke's shift observed from the N-CDs, dispersed in polar and non-polar solvents, as a function of temperature. Similar shifts were observed with hygroscopic solvents.

3.5 PL decay lifetime of N-CD in laboratory grade and dehydrated acetone

A comparative study of the PL decay- lifetime, at an excitation wavelength of 405 nm, from different solvent dispersions of N-CD is shown in Figure S5. Exponential decay functions were used to fit the lifetimes obtained from the different dispersions with $1.36 < \chi^2 < 1.25$ indicating a good fit. The exponential decay coefficients and their corresponding time constants are presented in Table3. As reported in a recent study, the N-CD showed a bi-exponential decay fit that suggests the occurrence of two distinct emissive states, which can be spectrally confirmed from the dual peaks obtained from the polar aprotic dispersions of N-CD[17].Both multi-exponential and single exponential decay fits were reported for N-CD[17,35].

Solvent	$\tau 1$	A1	$\tau 2$	A2	$\chi 2$
Water	4.13 ns	34.06	11.28 ns	63.3	1.36
Acetone(water removed)	1.36 ns	79.62	7.9 ns	20.38	1.34
Laboratory-grade Acetone	1.95 ns	33.93	10.22 ns	57.31	1.31
Ethyl Acetate	3.74 ns	41.33	9.81 ns	52.54	1.25

Table 3. Excited state lifetime values (τ), relative amplitudes (A) and chi-square value (χ) for the N-CD dispersed in various solvents

N-CD in hydrated acetone showed a much higher lifetime than its dehydrated part, as can be seen in Fig. 6. The water absorbed by the hygroscopic acetone results in the formation of a passivation layer formed by an aqueous shell around the carbon nano-dots. The longer lifetime observed with laboratory grade acetone may be due to the protection from the interaction of hydrogen-bond donor groups present on the carbon nano-dots and the solvent molecules. An increase in the non- radiative decay of the excited electrons, where they lose energy to the surrounding solvent, is impeded by the aqueous passivation layer resulting in a higher lifetime[13].Such observations further reveal the role of hydrogen bonds in controlling the PL of the N-CD.
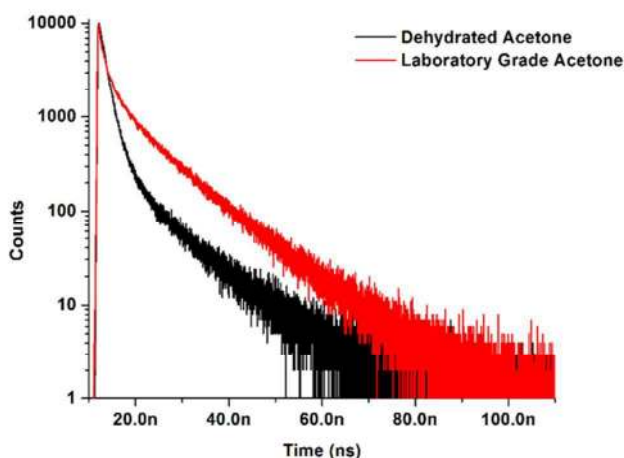
Fig. 6: Lifetime measurement of N-CDs dispersed in laboratory-grade and dehydrated acetone. A decrease in the lifetime of the N-CDs was observed when dehydrated acetone was the dispersant.λmax = 405 nm

3.6 Quantum Yield of N-CD dispersed in different solvents

The quantum yield (QY) of different solvent dispersions of the synthesized N-CDs were calculated (ESI; S6) at an excitation wavelength of 350 nm and has been tabulated in Table 4. An exponential dependence of QY on the permittivity of the dispersant can be observed (Fig. S6) that is in accordance to a recent study[36] while a second degree relation is seen between the PL intensity and the refractive index (η) of the dispersant, that can be related to the QY calculation (S6).The radiative rate for the N-CD dispersions was calculated according to the following equation[36]:

$$k = \frac{\phi}{\tau}$$ (3)

where *k, φ and τ* are the radiative rate, quantum yield and the PL decay lifetime of N-CDs dispersed in different solvents.

This radiative rate increased from 0.5×10^7 s^{-1} to 1.06×10^7 s^{-1}for acetone dispersions as compared to

the aqueous dispersions. Relaxation of energy via non-radiative pathways when surrounded by solvent

molecules of higher dielectric constant may result in this poor PL-QY. This reduction in the non-radiative

rate results in an increased PL efficiency. Further, studies on the effect of permittivity of the solvents on

the PL-QY is required.

Solvent	Permittivity (ε_0)	Refractive index (η)	Viscosity(μ) (centi-poise)	Quantum Yield (%)
Water	80.1	1.33	0.89	2.1
DMSO	46.7	1.47	1.99	7.1
Methanol	32.7	1.32	0.54	7.6
Acetone	20.7	1.35	0.32	8.6
Iso-propyl alcohol	17.9	1.37	2.1	9.6
Tetrahydrofuran	7.58	1.4	0.46	13.9

Table 4. Quantum yield of N-CDs dispersed in different solvents as a function of permittivity (ε_0), refractive index (η) and viscosity (μ).

3.7 Use of N-CDs to measure water content in polar aprotic solvents

This study can further be extended to quantify the amount of water present in polar aprotic and

hygroscopic solvents like acetone. The content of water in anhydrous acetone was increased

systematically with its percentage varying from 0.2% to 30% and was monitored through the emission

spectra of the N-CDs. On excitation at 380 nm, spectral shifts were observed with a decrease in the blue

emission intensity and an increase in its green emission when the water content was increased to 5%, as

shown in Fig. 7a. Fig. 7b illustrates the sensitivity of the N-CDs in detecting the water content in acetone,

that was calculated by normalizing the PL intensity at varying water concentrations with the blank (0.2 %

water). Saturation in emission intensity was reached at higher water concentrations that may be due to

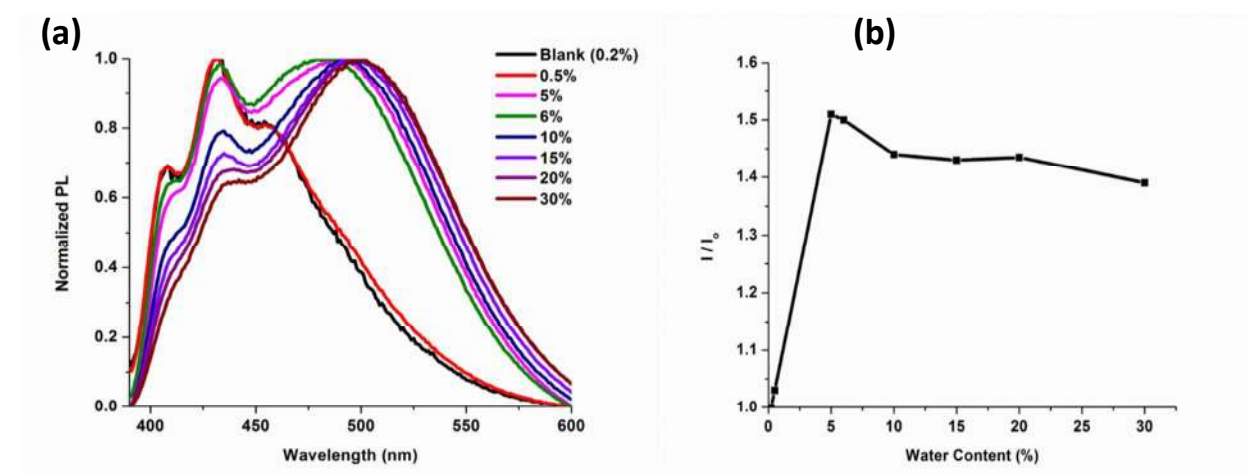the N-CDs being saturated by the aqueous solvent cage.

Fig. 7: (a) Spectral shifts observed with N-CDs dispersed in acetone with varying water content. (b) Normalized PL intensity (sensitivity) of the N-CDs to varying concentrations of water in acetone.

4. CONCLUSION

In conclusion, we have shown that both Lippert- Mataga model and Kamlet-Tafts parameters are

required to satisfactorily explain the photophysical properties of the dispersed N-CD wherein both

specific and non-specific interactions are involved. Spectral shifts associated with both absorption and

PL depends on the ability of different functional groups, present along the surface of the N-CD, to form

hydrogen bonds with the solvents. Such specific interactions act as a primary driving force in controlling

the distance between the N-CD and the solvent molecules which again play a role in influencing its

photophysical properties. However, in the absence of hydrogen bonds, dipole interactions are

predominant. This was supported by a mathematical model which was dependent on the Kamlet-Taft's

parameters of the solvent molecules. Results also show that PL quantum yield of the N-CDs can be regulated by the refractive index and permittivity of the solvent. An increase in the radiative rate increases the PL efficiency of the N-CDs when dispersed in acetone as compared to water. Owing to the sensitivity of these N- CDs towards low concentrations of water, these nano-dots can further be used as a sensitive humidity sensor.

ACKNOWLEDGEMENT

SUPPORTING INFORMATION DESCRIPTION

It contains the synthesis of the N-CD by MWAH method wherein citric acid and urea were used as precursors. Characterization techniques and their interpretation are also been included.Derivation of the mathematical model used to infer the spectral shifts observed with the absorption spectra of the N-CD.Lifetime decay spectra and a graphical interpretation of the formation of an aqueous shell around the N-CD in polar protic and hygroscopic aprotic solvents are also included.

Physical Chemistry Chemical Physics Accepted Manuscript

REFERENCES

1.K. Schroeder, R. Goreham andT. Nann,*Pharm Res,* 2016,**33**, 2337-2357.

2.R. Xie, Z. Wang, W. Zhou, Y. Liu, L. Fan, Y. Li and X. Li,*Anal. Methods,* 2016,**8**, 4001-4016.

3.J. Kim, S.Kim, M. Park, S. Bae, S. Cho, Q. Du, D. Wang, J. Park and B.Hong*Sci. Rep.,* 2015,**5**, 14276.

4.X. Yan,X. Cui, B. Li and L. Li,*Nano Lett,* 2010, **10**, 1869-1873.

5.L. Tang, R. Ji, X. Cao, J. Lin, H. Jiang, X. Li, K. Teng, C. Luk, S. Zeng and J. Hao,*et al.ACS Nano*, 2012, **6**, 5102-5110.

6.Y. Liu Y., Kim D. Ultraviolet And Blue Emitting Graphene Quantum Dots Synthesized from Carbon Nano-Onions and their Comparison for Metal Ion Sensing. *Chem. Commun.*, 2015, **51**, 4176-4179.

7.A. Sharma, T. Gadly, A. Gupta, A. Ballal, S. Ghosh, and M. Kumbhakar,*J. Phys. Chem. Lett.* 2016, **7**, 3695-3702.

8.S. Hu, A. Trinchi, P. Atkin,and I. Cole ,*Angew. Chem.* 2015; **54**, 2970-2974.

9.Y. Zhao, X. Liu, Y. Yang, L. Kang, Z. Yang, W. Liu and L. Chen,*Fuller. Nanotub Car N.*, 2015,**23**, 922-929.

10.Q. Xu, J. Zhao, Y. Liu, P. Pu, X. Wang, Y. Chen, C. Gao, J. Chen and H. Zhou,*J. Mater. Sci. Lett.*, 2015,**50**, 2571-2576.

11.C. Sun, Y. Zhang, P. Wang, Y. Yang, Y. Wang, J. Xu, Y. Wang and W. Yu,*Nanoscale Res Lett*, 2016; **11**, 1326- 1328.

12.S. Cushing, M. Li, F. Huang,and N. Wu,*ACS Nano,*2014, **8**, 1002-1013.

13. Gan Z., Xu H., Hao Y. Mechanism For Excitation-Dependent Photoluminescence from Graphene Quantum Dots and other Graphene Oxide Derivates: Consensus, Debates and Challenges. Nanoscale 2016; 8: 7794-7807.

14.S. Khan, A. Gupta, N. Verma and C. Nandi,*Nano Lett.*, 2015,**15**, 8300-8305.

15.K. Habiba, V. Makarov, J. Avalos,M. Guinel, B. Weiner and G. Morell,*Carbon*, 2013,**64**, 341-350.

16.D.Qu, M. Zheng, J. Z. Li,Z. Xie and Z. Sun, *Light: Science & Applications,* 2015,**4**, e364_1 – e364_8.

17.A. Sciortino, E. Marino, B. Dam, P. Schall, M. Cannas and F. Messina,*J. Phys. Chem. Lett.*, 2016,**7**, 3419-3423.

18.D. Qu, M. Zheng, L. Zhang, H. Zhao, Z. Xie,X. Jing, R. Haddad, H. Fan and Z.Sun,*Sci. Rep.* 2014,**4**, 5294_1- 5294_9.

19.X. Liu, J. Pang, F. Xu, and X. Zhang,*Sci. Rep.* 2016, **6**, 31100_1- 31100_8.

20.L. Li, L. Li, C. Wang, K. Liu, R. Zhu, H. Qiang and Y. Lin,*Microchimica Acta,* 2014,**182**, 763-770.

21.D. Jiang,Y. Chen,N. Li,W. Li, Z. Wang,J. Zhu,H. Zhang,B. Liu and S. Xu,*PLoS ONE,* 2015,**10**, e0144906_1- e0144906_15.

22.R. Jones , *Chem. Rev.,* 1943,**32**, 1-46.

23Y. LLi, H. Zhang, M. Crespo, H. Porwal, O. Picot, G. Santagiuliana, Z. Huang, E. Barbieri, N. Pugno, and T. Peijs,*et al.ACS Appl. Mater. Interfaces,* 2016,**8**, 24112-24122.

24.X.Wu, F.Tian, W. Wang, J. Chen, M.Wu and J. Zhao,*J. Mater. Chem. C,* 2013**, 1**, 4676- 4676.

25.X. Li, Z. Zhou, D. Lu, X. Dong, M. Xu, L. Wei and Y. Zhang,*Nanoscale Res Lett,* 2014,**9**, 583_1- 583_6.

26. L. Li,G. Wu, G. Yang, J. Peng, J. Zhao and J. Zhu, *Nanoscale,* 2013**, 5**, 4015-4039.

27 C. Reckmeier, Y. Wang, R. Zboril, andA. Rogach,*J. Phys. Chem. C,* 2016, **120**, 10591-10604.

28. S. Schulman, Fluorescence and Phosphorescence Spectroscopy, Pergamon Press: New York, 1977.

29. T. Haldar, and S. Bagchi, *J. Phys. Chem. Lett.,* 2016, **7**, 2270-2275.

30. X. Wang, L. Cao, F. Lu, M. Meziani, H. Li, G. Qi, B. Zhou, B. Harruff, F. Kermarrec and Y. Sun,*Chem. Commun.,* 2009, 3774-3776

31. Natelson, D. Nanostructures And Nanotechnology, Cambridge University Press, 2015.

32. B. Razbirin, N. Rozhkova, E. Sheka, D. Nelson, A. Starukhin,*J. Exp. Theor. Phys*., 2014,**118**, 735-746.

33. T. Fan, Zeng W., Tang W., Yuan C., Tong S., Cai K., Liu Y., Huang W., Min Y., Epstein A. *Nanoscale Res Lett,* 2015,**10**, 55_1- 55_8.

34. F. Zhang, F. Liu, C. Wang, X. Xin, J. Liu, S. Guo andJ. Zhang, *ACS Appl. Mater. Interfaces*, 2016; **8**, 2104-2110.

35. M. Röding, S. Bradley, M. Nydén and T. Nann,*J. Phys. Chem. C*, 2014,**118**, 30282-30290.

36 Z. Liu, Z. Wu, M. Gao, H. Liu, C. Huang.*Chem. Commun.* 2016, *52,* 2063-2066.